Cerebral Cortex, 2021;00: 1–14

https://doi.org/10.1093/cercor/bhab393
Original Article

ORIGINAL ARTICLE

Long-Term Stress and Trait Anxiety Affect Brain Network Balance in Dynamic Cognitive Computations

Liangying Liu[1,2,†], Jianhui Wu[3,†], Haiyang Geng[1,3], Chao Liu[1,3], Yuejia Luo[1,3,4], Jing Luo[5] and Shaozheng Qin[1,2,6]

[1]State Key Laboratory of Cognitive Neuroscience and Learning & IDG/McGovern Institute for Brain Research, Faculty of Psychology at Beijing Normal University, Beijing 100875, China, [2]Beijing Key Laboratory of Brain Imaging and Connectomics, Beijing Normal University, Beijing 100875, China, [3]Center for Brain Disorder and Cognitive Science, Shenzhen University, Shenzhen 518061, China, [4]Center for Emotion and Brain, Shenzhen Institute of Neuroscience, Shenzhen 518061, China, [5]School of Psychology, Capital Normal University, Beijing 100048, China and [6]Chinese Institute for Brain Research, Beijing 102206, China

Address correspondence to Shaozheng Qin, IDG/McGovern Institute for Brain Research, Beijing Normal University, 19 Xinjiekouwai Street, Beijing 100875, China. Email: szqin@bnu.edu.cn
[†]L.L. and J.W. contributed equally to this work

Abstract

Long-term stress has a profound impact on executive functions. Trait anxiety is recognized as a vulnerable factor accounting for stress-induced adaptive or maladaptive effects. However, the neurocognitive mechanisms underlying long-term stress and trait anxiety interactions remain elusive. Here we investigated how long-term stress and trait anxiety interact to affect dynamic decisions during n-back task performance by altering functional brain network balance. In comparison to controls, participants under long-term stress experienced higher psychological distress and exhibited faster evidence accumulation but had a lower decision-threshold when performing n-back tasks in general. This corresponded with hyper-activation in the anterior insula, less deactivation in the default-mode network, and stronger default-mode network decoupling with the frontoparietal network. Critically, high trait anxiety under long-term stress led to slower evidence accumulation through higher frontoparietal activity during cognitively demanding task, and increased decoupling between the default-mode and frontoparietal networks. Our findings suggest a neurocognitive model of how long-term stress and trait anxiety interplay to affect latent dynamic computations in executive functioning with adaptive and maladaptive changes, and inform personalized assessments and preventions for stress vulnerability.

Key words: anxiety, dynamic decision, functional magnetic resonance imaging, network balance, stress

Introduction

Now, more than ever, increasing exposure to psychosocial stress has become an unavoidable part of our contemporary society as the pace of life rapidly accelerates. Exposure to sustained stress can have a profound impact on the brain and cognition through activation of stress-sensitive neuromodulatory systems and the release of stress hormones (de Kloet et al. 2005; Arnsten 2009). The adverse effects of long-term stress on executive functions are widely documented (Arnsten 2009; Lupien et al. 2009). Yet, long-term stress has also been associated with no impairment or even enhanced cognitive functions (Joëls et al. 2006). Thus, long-term stress can lead to either beneficial forms of learning that promote adaptation or detrimental effects that presage maladaptation, likely depending on the level of stress resilience or vulnerability of each individual (Franklin et al. 2012; McEwen and Morrison 2013). Trait anxiety, a stable disposition to interpret a wide range of environmental events in a negative way, has been recognized as a vulnerable factor (Bishop and Forster 2013; Weger and Sandi 2018), which could account for the seemingly paradoxical effects of stress. Neurocognitive models of human anxiety suggest that high trait-anxious individuals tend

to make additional effort to prevent shortfalls in performance effectiveness (i.e., accuracy) with deficits becoming evidence in processing efficiency (i.e., reaction times, RTs) on tasks involving executive function and deliberate dynamic decision processing (Calvo et al. 1994; Calvo 1996; Edwards et al. 2015). However, how trait anxiety and long-term stress interact to affect dynamic decisions during n-back task remains unclear. Considering both long-term stress and trait anxiety provides a better understanding of the profound effects of long-term stress on the brain and cognition than either in isolation.

Recent advances in computational modeling of trial-by-trial decision making enable us to identify latent dynamic computations in various cognitive domains including executive functions (Bishop 2007; Browning et al. 2015; Xu et al., 2021). The architecture of executive function includes several main components like working memory, selective attention, and cognitive inhibition (Diamond 2013). One of the most widely used paradigms for measurement of executive functions in human studies is the n-back task (Kane and Engle 2002; Conway et al. 2005). Research in sequential-sampling theory thus posits that the n-back task, analogous to speeded decision-making, can be modeled as an evidence accumulation process during which effective information (namely evidence) extracted from a stream of inherently noisy observations are rapidly accumulated until sufficient evidence reaches the threshold to make a decision and the choice response is then executed (Ratcliff 1978). Drift diffusion model (DDM), in particular, is used to decompose participant's choice responses in a given task into latent decision-making dynamics modulated by free parameters. Of these parameters, the speed of evidence accumulation refers to "drift rate" reflecting the ability to extract effective information from perceived inputs (Ratcliff and McKoon 2008). The frontalparietal network (FPN) regions, particularly the dorsolateral prefrontal cortex (dlPFC) in the middle frontal gyrus (MFG) and the inferior parietal sulcus (IPS), are responsible for evidence accumulation in humans and nonhuman primates (Mulder et al. 2014). These regions are also the major targets of stress hormones such as glucocorticoids and catecholamines through which neuronal excitability and network connectivity are affected (Birnbaum et al. 2004; Wang et al. 2007; Xiong et al. 2021). As a vulnerable phenotype of stress-related mental illness, high trait anxiety has been linked to deficient processing efficiency anchored onto the FPN critical for executive function (Bishop 2009). Yet, how long-term stress and trait anxiety interact to affect the FPN in the dynamic decision process remains open.

The engagement of FPN regions during executive function tasks is usually accompanied by disengagement of core regions of the default mode network (DMN), especially the posterior cingulate cortex (PCC) and medial prefrontal cortex. These DMN regions have been implicated into mind-wandering and allocation of resources to internal thoughts (Raichle et al. 2001). Less DMN deactivation has been observed under acute stress and anxious individuals (Menon 2011), implying deficient reallocation of resources from internal thoughts to external tasks. Moreover, the salience network (SN) has been implicated in triggering a shift of neurocognitive resources to prioritize affective processing over deliberate executive functions (Luo et al. 2014). Indeed, hyper-activation in the anterior insula and dorsal anterior cingulate cortex (dACC), core nodes of the SN, has been seen in anxious individuals (Raichle et al. 2001). Although reduced disengagement of the DMN and hyper-activation in the SN are observed under acute stress (Qin et al. 2009), whether or not sustained exposure to stress leads to a similar effect on the DMN and SN remains unclear.

Beyond local activation, human executive functions rely on nuanced functional coordination among large-scale brain networks of the FPN, SN, and DMN to support constantly maintaining and updating of relevant information according to ever-changing cognitive/environmental demands. In particular, functional decoupling between the FPN and DMN plays a crucial role in support of goal-directed tasks by suppressing task-irrelevant internal thoughts (Cocchi et al. 2013; Liu et al. 2016). The SN is believed to be responsible for regulating a balance between FPN engagement and DMN disengagement to facilitate access to externally oriented stimuli and inhibit internally oriented attention during cognitively demanding task (Sridharan et al. 2008). Unbalanced functional organization of these networks, with either hypo- or hyper-connectivity, has been seen in anxious individuals or under acute stress (Bishop 2007; Hermans et al. 2014). However, how trait anxiety modulates the effects of long-term stress on functional balance of these networks during higher-level cognitive task remains open.

Here we address the questions proposed above by leveraging functional magnetic resonance imaging (fMRI) and computational modeling of trial-by-trial decision responses to investigate how long-term stress and trait anxiety interact to affect dynamic decision computations during n-back task (Fig. 1*a*). In the long-term stress group, participants were recruited from those who have been preparing for the upcoming competitive Chinese National Postgraduate Entrance Exam (CNPEE) for at least 6 months. Exposure to such an exam has been proven as a natural long-term psychosocial stressor by our and other laboratories (Duan et al. 2013, 2015). In the control group, participants matched in age and education who were not preparing for the CNPEE and did not have exposure to other major stressors in past 6 months were recruited. Participants underwent fMRI scanning while performing a numerical n-back task consisting of 0- and 2-back conditions (Fig. 1*b*). Trait anxiety and psychological distress were assessed 1 day before the fMRI experiment. A Bayesian hierarchical version of the drift diffusion model (HDDM) was implemented to estimate latent dynamic decision parameters during task processing. Brain activation and network approaches were employed to identify how long-term stress and trait anxiety alter functional brain network balance. Based on neurocognitive models of stress and anxiety, we expected that individual differences in trait anxiety would modulate the effects of long-term stress on latent dynamic decisions during n-back task, likely involving altered brain functional balance among the FPN, DMN, and SN regions at activation, deactivation, and network coupling levels.

Methods and Materials

Participants

Seventy-two healthy male senior college students participated in this study. The sample size in this study is based on our previous fMRI and ERP studies on acute stress (Qin et al. 2012a, 2012b) and long-term stress (Wu et al. 2014). Thirty-eight participants (age range: 20–24 years old, mean ± standard deviation (SD) = 21.57 ± 0.83) in the long-term stress group were recruited 1–3 weeks before a highly competitive CNPEE. An independent cohort of 34 male participants matched in age and education who did not participate in the CNPEE or have any

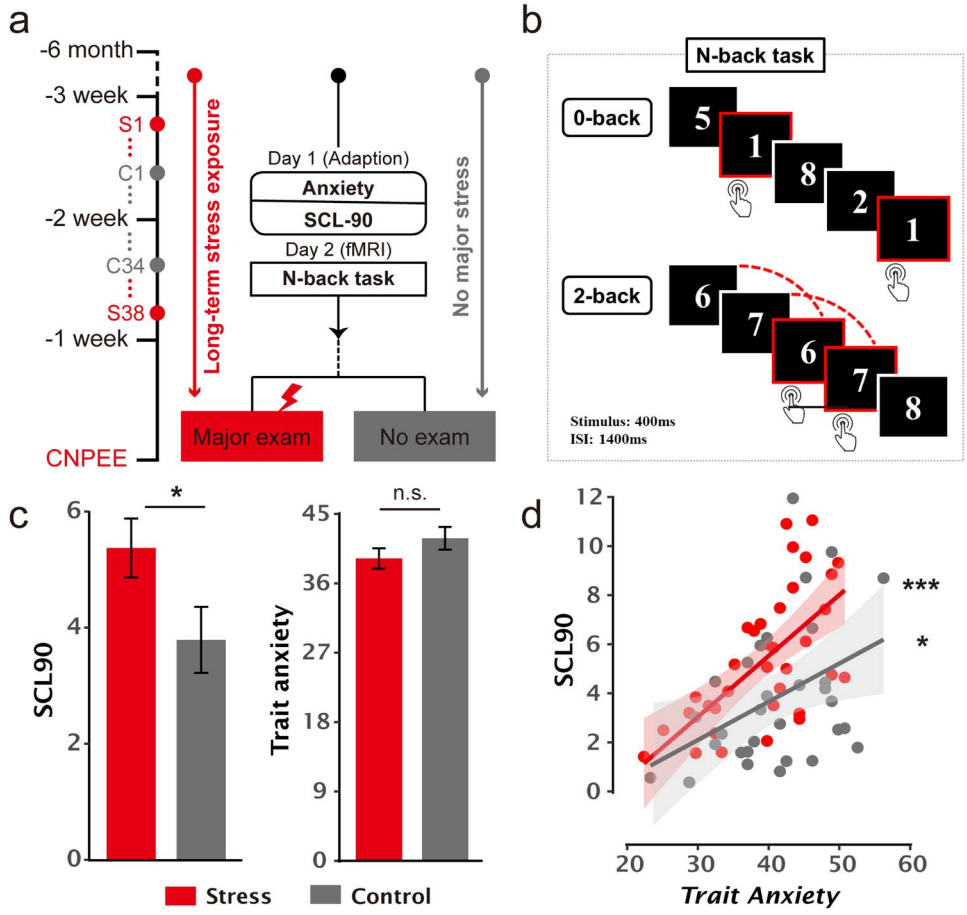

Figure 1. Experimental design and the effects of trait anxiety on psychological distress measurements among long-term stress and control groups. (*a*) An overview of experimental design illustrates the major procedures for participants from long-term stress and control groups with trait anxiety and SCL-90 assessments on the adaptation day (Day 1) before the fMRI n-back task (Day 2). These assessments occurred 1–3 weeks before the major exam stressor. There were 38 participants (S38) in the long-term tress group and 34 (C34) in the control group. Two participants from each group were excluded from further analyses due to excessive head motion during fMRI scanning, resulting in 36 and 32 participants in the stress and control groups, respectively (*b*) An illustration of the numerical n-back task that consists of 0- and 2-back conditions, with each digit item presented for 400 ms followed by an interstimulus interval of 1400 ms. Participants were instructed to detect whether the current item was "1" in the 0-back condition and were asked to decide whether the current item had appeared 2 positions back in the sequence in the 2-back condition. (*c*) Bar graphs depict psychological distress measured by the SCL-90 scores and trait anxiety in the long-term stress and control groups. Psychological distress measured by SCL90 significantly differed between stress and control groups. (*d*) Positive correlations of psychological distress with trait anxiety in long-term stress and control groups. ***$P < 0.001$, *$P < 0.05$; n.s., not significant.

other anticipated stressor were recruited to the control group. Informed written consent was obtained from all participants before the experiment, and the study protocol was approved by the Institutional Review Board for Human Subjects at Beijing Normal University. Inclusion criteria for long-term exam stress were as follows (Supplementary Fig. S1): 1) Participants had been preparing for the upcoming competitive CNPEE for at least 6 months. 2) Participants had to provide the CNPEE certificate registered more than 6 months before the experiment. 3) They had to participate the experiment within a 1- to 3-week time window before the CNPEE to ensure that they were experiencing high levels of psychosocial stress. We did not included female participants to mitigate potential confounds of their menstrual cycles (Etkin and Wager 2007). Four participants (2 in each group) were excluded from further analyses due to head movement >1 voxel in translation or in rotation. Informed written consent was obtained from all participants before the experiment, and the study protocol was approved by the Institutional Review Board for Human Subjects at Beijing Normal University. Four participants (2 in each group) were excluded from further analyses due to head movement >1 voxel in translation or in rotation.

General Experimental Procedure and N-Back Task

Both psychological distress and trait anxiety measures were administrated 1 day before the fMRI experiment to mitigate potential confounding effects for their self-reports that may suffer from bias during times of acute stress in the task experiment. On the experimental day, participants were instructed to practice the task before fMRI scanning (Liston et al. 2009). We used the 0- and 2-back conditions only to create a robust contrast between low- and high-task demands to gain the differences in modeling parameters, brain activation, and connectivity measures between these 2 conditions.

The entire n-back task included 10 blocks, which alternated between 5 0-back blocks and 5 2-back blocks, interleaved by a jittered fixation that ranged from 8 to 12 s (Fig. 1b). When detecting a target, participants were required to press a button

with their index finger as quickly and accurately as possible, and to withhold their response for target-absent trials. There were 21 targets and 17 targets for the 0- and 2-back conditions, respectively.

Psychological Measurements of Long-Term Stress

The State–Trait Anxiety Inventory (1985), one of the most commonly used scales to measure trait anxiety level in healthy populations, was collected both in the stress and control groups (Supplementary Fig. S2). The Symptom Checklist (SCL-90) was used to evaluate psychological distress including symptoms of psychopathology under long-term stress (Derogatis and Unger 2010). Each item of the questionnaire is rated on a 5-point scale of distress from 0 (none) to 4 (extreme). The SCL-90 consists of the following 9 primary symptom dimensions: somatization, obsessive–compulsive, interpersonal sensitivity, depression, anxiety, hostility, phobic anxiety, paranoid ideation and psychoticism. Each of the 9 symptom dimensions comprises 6–13 items. We compute the average score for each symptom dimension and then sum these 9 mean scores as the global indices for each participant. Scores for each subscale of the SCL-90 are indeed ranging from 0 to 23 for participants in both groups (Supplementary Fig. S12). One outlier larger than 2.5 standard deviations from the control group was excluded for SCL data.

HDDM for Estimating Latent Decision Parameters during N-Back Task

The DDM conceptualizes decision-making as an evidence accumulation process in which effective evidence is extracted from the representations of stimuli that are inherently variable and noisy and gradually accumulated over time until sufficient evidence reaches the decision threshold and a choice is executed (Fig. 2a). For the n-back task, such evidence accumulation process can be considered as accumulating effective information in mind on the exact position of each item to make a precise decision whether the current item appeared 2 positions back in the sequence. The DDM was then implemented to decompose participants' trial-by-trial RTs into latent processes which were modulated by the following free parameters: 1) drift rate v, 2) decision threshold a, 3) nondecision time t, 4) starting point z (Wiecki et al. 2013).

The DDM is known as a de facto standard for the two-alternative forced choice tasks, in which the 2 choices correspond to the upper and lower decision boundaries, respectively (Ratcliff and McKoon 2007). Recent advances have extended the DDM to many task paradigms with 1 choice such as Go/no-Go task, as RTs of no-Go condition cannot be measured (Zhang et al. 2015; Ratcliff et al. 2018). Likewise, we fitted the DDM to trial-by-trial RTs for hits (target items with successful response) and false alarms (nontarget trials with response) in 0- and 2-back conditions. The DDM parameters were then estimated by the HDDM across participants for its suitability to a relatively small number of trials, according to the most recent simulation data by systematic comparisons of multiple drift models (Lerche et al. 2017). Critically, the hierarchical modeling formulated in the Bayesian framework allows us to simultaneously estimate parameters on both group and individual levels, in a way that individual parameters were drawn from the group distribution (Wiecki et al. 2013). Differences in RTs between 0- and 2-back conditions, and between stress and control groups, implicate changes in 1 or more DDM parameters between task conditions

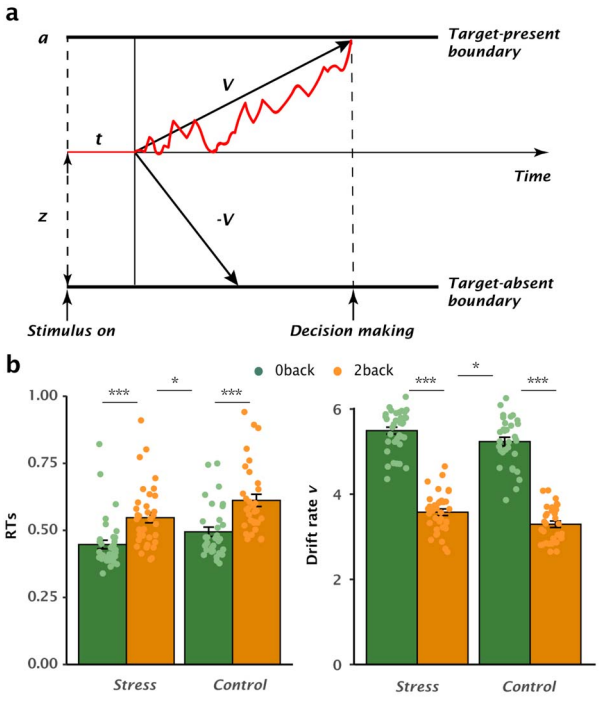

Figure 2. Effects of long-term stress on latent dynamic decision-making during n-back task. (*a*) Schematic view of the drift diffusion model accounting for the n-back task with 4 model parameters: Drift rate (v) indicates the rate of evidence accumulation until boundary threshold a is reached. The nondecision time t represents the time for stimulus encoding in addition to decision-making process. The starting point z reflects the prior preference toward 1 choice over the other. (*b*) Left: Mean reaction times for 0- and 2-back conditions in the stress and control groups. Right: Estimated model parameter for drift rate in the DDM. Notes: Error bars represents SEM. Dots represent individual parameters.

and groups. To examine whether the 4 parameters varying 0- and 2-back conditions led to greater biases between different models, 15 variants of the DDM with different parameter constraints were established for both stress and control groups (Supplementary Fig. S4). Model comparisons were conducted by using deviance information criterion (DIC) (Supplementary Table S22) (Wiecki et al. 2013). For each model, Markov chain Monte Carlo (MCMC) sampling methods were applied to perform Bayesian inference by generating 20 000 samples and discarding the first 2000 samples as burn-in. The best model is determined by the minimum DIC. We further employed the Gelman–Rubin statistic to assess the convergence of the model. Note that a difference of 10 in DIC is considered acceptable (Zhang and Rowe 2014). The value of $\hat{R}$ computed for all parameters was close to 1.0 and < 1.01, indicating good convergence where successful convergence is indicated by values < 1.1 (Wiecki et al. 2013). The 4 parameters of each participant from the best fitted model were then submitted to subsequent analyses.

Behavioral Data Analysis

Two-sample t-tests were conducted to compare the differences in trait anxiety and psychological distress between groups. Correlation analyses were conducted to compute the relationships of trait anxiety with psychological distress and latent dynamic decision measures from HDDM. Statistical tests were conducted

to compare group differences in Fisher *r*-to-*z*-transformed correlation coefficients. Separate analyses of variance (ANOVAs) were conducted to examine the effects of long-term stress on conventional and latent computational measures for the 0-back and 2-back conditions. Mixed factorial ANOVAs were conducted using the "afex" R package (Singmann et al. 2016), and the Greenhouse–Geisser correction was applied whenever a nonsphericity assumption was violated. For regressions and multigroup structural equation models (SEMs), the Pearson's coefficient *r* and estimated coefficients *indirect Est* are used as effect size. According to Cohen, the effect size is low if the value of *r* varies around 0.1, medium if *r* varies around 0.3, and large if *r* varies > 0.5 (Cohen 2013). Cohen's *d* and *q* are employed to measure effect size respectively for 2 independent *t*-test and the difference between 2 correlations (Cohen 2013). Cohen suggested that $d = 0.2$ could be considered as a "small" effect size, 0.5 represents a "medium" effect size and 0.8 as a "large" effect size. Cohen proposed the following categories for the *q* interpretation: < 0.1: no effect; 0.1 to 0.3: small effect; 0.3 to 0.5: intermediate effect; > 0.5: large effect. Generalized eta squared (η^2_g) is used as a measure of the effect size for our mixed 2-by-2 ANOVA. Usually, $\eta^2 = 0.01$ indicates a small effect; $\eta^2 = 0.06$ indicates a medium effect; $\eta^2 = 0.14$ indicates a large effect.

Imaging Data Acquisition

Participants were scanned in a Siemens 3.0-Tesla TRIO magnetic resonance imaging (MRI) scanner (Erlangen, Germany) at the Brain Imaging Center of the National Key Laboratory of Cognitive Neuroscience and Learning at Beijing Normal University. Functional images were acquired with a gradient-recalled echo planar imaging sequence (axial slices 33, repetition time 2000 ms, echo time 30 ms, flip angle 90°, slice thickness 4 mm, gap 0.6 mm, field of view 200 × 200 mm, and voxel size $3.1 \times 3.1 \times 4.6$ mm^3). Functional imaging session lasted 464 s during the n-back task. To improve individual coregistration and spatial normalization, a high-resolution anatomical image was acquired in the sagittal orientation using a T1-weighted 3D magnetization-prepared rapid gradient echo sequence (slices 192, repetition time 2530 ms, echo time 3.45 ms, flip angle 7°, slice thickness 1 mm, field of view 256 × 256 mm, and voxel size $1 \times 1 \times 1$ mm^3).

Imaging Data Analysis

Preprocessing

Imaging data analysis was performed using Statistical Parametric Mapping 8 (SPM8 https://www.fil.ion.ucl.ac.uk/spm/software/spm8/). The first 4 functional volumes were discarded to enable T1 equilibration. The remaining volumes were first realigned to correct for head motion. The realigned volumes were then corrected for slice acquisition timing. The mean functional image was coregistered to each participant's T1-weighted structural image and then normalized to a standard stereotaxic Montreal Neurological Institute (MNI) space with a resolution of $2 \times 2 \times 2$ mm^3. The functional images were then spatially smoothed by an isotropic Gaussian kernel with 6-mm full-width at half-maximum. Smoothed images were statistically analyzed under the general linear model (GLM) framework in SPM8.

GLM Analysis

To assess neural activity associated with 0-back and 2-back conditions, these conditions were modeled separately as boxcar regressors and convolved with the canonical hemodynamic response function built in SPM8. In addition, 6 realignment parameters from preprocessing were included to account for movement-related variability. The analysis included high-pass filtering using a cutoff of 1/128 Hz and a serial correlation correction using a first-order autoregressive model (AR[1]).

Corresponding contrast parameter images for 0- and 2-back conditions at the individual level were then submitted to a second-level group analysis using 2-by-2 factorial ANOVA, with Group (long-term stress vs. control) as between-subject factor and white matter (WM)-load (0- vs. 2-back) as within-subject factor to examine the main effects of Group and WM-load, and their interaction on task-invoked brain response. We identified brain regions showing significant Group and WM-by-Group interaction effects, and then applied a conjunction analysis of the minimum statistic (Nichols et al. 2005) with the contrasts of "2- > 0-back" and "0- > 2-back" separately. This allows us to identify brain regions commonly showing WM-by-Group interaction and WM-related activation/deactivation. Significant clusters were determined by a voxel-wise height threshold of $P < 0.001$ and an extent threshold of $P < 0.05$ corrected for multiple comparisons using suprathreshold cluster-size approach based on Monte-Carlo simulations (Supplementary Table S6). Given our priori hypotheses regarding the DMN, SN, and FPN regions, these regions were additionally investigated using a height threshold of $P < 0.005$ and an extent threshold of $P < 0.05$ corrected for multiple comparisons. Monte-Carlo simulations were implemented using the AlphaSim procedure. Ten thousand iterations of random 3D images, with the same resolution, dimensions and 6-mm smoothing kernel as used our fMRI data analysis, were generated. The maximum cluster size was then computed for each iteration and the probability distribution was estimated across the 10 000 iterations. This approach allowed us to determine the minimum cluster size that controls for false-positive rate for regions of interest. Parameter estimates were extracted from significant clusters to characterize task-invoked response as a function of WM-load, trait anxiety and groups using 3dmaskave built in AFNI.

Given the prominent effect of long-term stress on drift rate in the 2-back condition, we then focused on neural correlates of drift rate in long-term stress and control groups in the following analyses (Supplementary Figs S9 and S10). To identify brain regions showing the interaction effects between group and drift rate, two-sample *t*-test was conducted for contrast images of the 2-back condition by treating drift rate as a continuous covariate with no mean centering (analogous to ACNOVA). In addition, we also examined executive functions-related brain activity associated with drift rate but not necessarily interacting with groups, which might exhibit the mediation effects in the long-term stress different from controls. Whole-brain regression analysis was then conducted to search for the neural correlates of drift rate in the 2-back condition in the stress group (Supplementary Fig. S10 and Tables S15-S16). Significant clusters were determined by the same criteria as noted above and corresponding parameter estimates were then extracted. Once associations between drift rate and brain activation were identified, we then conducted correlation analyses to examine whether such brain activation was also associated with individual differences in trait anxiety for both 2 groups. If executive functions-related brain activity was correlated with both drift rate and trait anxiety, SEMs were then constructed to examine the potential mediation effects of executive functions-related brain activity in these regions.

Prediction Analysis

Prediction analyses were performed by Python package "sklearn," using a machine learning approach with balanced 4-fold cross-validation with 4 repeats combined with linear regression to confirm the conventional correlations (Cohen 2010). The 4-fold cross-validation procedure was used to avoid overfitting that can occur when the leave-one-out cross-validation procedure is used on small sample sizes. We first estimated $r_{(\text{predicted, observed})}$, the correlation between the values predicted by the regression model and the observed/actual values, using a balanced 4-fold cross-validation procedure. The $r_{(\text{predicted, observed})}$ is a measure of how well the independent variable(s) predict the dependent variable. Data were divided into 4-folds such that the distributions of dependent and independent variables were balanced across folds. A linear regression model was built using 3-folds, leaving out 1-fold. The samples in the left-out fold were then predicted using this model, and the predicted values were noted. This procedure was repeated 4 times, and finally an $r_{(\text{predicted, observed})}$ was computed based on the predicted and observed values. Finally, the statistical significance of the model was assessed using nonparametric analysis. The empirical null distribution of $r_{(\text{predicted, observed})}$ was estimated by generating 500 surrogate datasets under the null hypothesis that there was no association between independent and dependent variables. Each surrogate dataset Di of size equal to the observed dataset was generated by permuting the labels (dependent variables) on the observed data points. $r_{(\text{predicted, observed})\text{i}}$ was computed using the actual labels of Di and predicted labels using the 4-fold cross-validation procedure described previously. This procedure produces a null distribution of $r_{(\text{predicted, observed})}$ for the regression model. The statistical significance of the model was then determined by counting the number of $r_{(\text{predicted, observed})\text{i}}$ greater than $r_{(\text{predicted, observed})}$ and then dividing that count by the number of Di datasets (500 in our case).

SEM

Separate multigroup SEMs were conducted via MPLUS 7.4 (Hayes et al. 2011) to test the mediating effects of executive task-related activity (i.e., IPS and MFG) on the association between trait anxiety and drift rate in long-term stress and control groups. Both direct and indirect effects of 2 groups and their group differences were estimated using 95% bias-corrected confidence intervals (CIs) with 10 000 bootstrapped resamples (Preacher and Hayes 2008). The 95% bias-corrected CIs without the inclusion of 0 indicate a statistically significant indirect effect at $P < 0.05$ (Preacher and Hayes 2008). Several fit indices evaluating the fitness of the proposed models were provided and used the following guidelines for judging good fit: The root mean square error of approximation (RMSEA) is considered adequate below 0.08. The standardized root mean square residual (SRMR) refers to the standardized difference between the observed correlation and the predicted correlation, and considered acceptable with values of 0.08 or less (Hu and Bentler 1999). The comparative fit index (CFI) considers the number of parameters, or paths, in the model and is considered good at 0.93 or above. Parallel analyses were further conducted for state anxiety.

Network Analysis for Task-State fMRI Data

Node Definition of Brain Networks

Core nodes of the typical FPN, DMN, and SN were derived from an automated meta-analysis of the most recent 11 406 fMRI studies in Neurosynth (http://www.neurosynth.org) (Yarkoni et al. 2011). The nodes in these 3 networks are presented in Figure 6*a*. Briefly, brain masks of the FPN, DMN, and SN were first generated using 3 separate terms of "working memory," "default mode," and "SN," respectively. The nodes of the FPN included the DLPFC and the IPS. The nodes in the DMN included the medial prefrontal cortex (MPFC) and the PCC, and the nodes in the SN included the dACC and the AI. Among these ROI masks, the MPFC, PPC, and dACC, locating at the middle line structures, form into their own joint clusters across both the left and right hemispheres. For the remaining masks, we combined the clusters from the left and right hemispheres into 1 unified mask, and time series from the left and right hemispheres were the averaged. The nodes were visualized with the BrainNetViewer (http://www.nitrc.org/projects/bnv/).

Intra and Internetwork Functional Connectivity

Task-specific (i.e., 2-back) ROI–ROI functional connectivity analysis were performed using the functional connectivity toolbox (CONN) toolbox (https://www.nitrc.org/projects/conn/) (Whitfield-Gabrieli and Nieto-Castanon 2012).

Our network coupling metrics derived from the CONN package actually assess functional connectivity between task-invoked time series of certain given regions in each condition separately. This measure is believed to reflect functional coupling among brain regions or nodes of interest under certain cognitive task. In this view, we thus feel that the 2-back condition alone rather than the difference between 2- vs. 0-back condition would be better to reflect FNP–DMN functional coupling, as the 0-back may not be optimal to serve as a baseline in the context of task-dependent functional connectivity. For each participant, 6 ROIs' averaged time series were generated as regressors of interest. Nuisance covariates including cerebrospinal fluid (CSF), WM, and movement parameters were regressed from the blood oxygen level–dependent (BOLD) signal using CompCor method implemented in CONN. Bivariate correlations were then computed between each pair of nodes, resulting in 6×6 correlation matrix for each participant in the 0-back and 2-back conditions separately (Supplementary Fig. S11).

Intra and internetwork functional connectivity metrics were computed separately. For each participant, the intranetwork connectivity strength in each condition was calculated by averaging Fisher z-transformed bivariate correlation coefficients between the weighted BOLD time series of nodes within each network. Correspondingly, the internetwork connectivity strength was computed by averaging Fisher z-transformed bivariate correlation coefficients of the weighted BOLD time series across nodes between 2 different networks. To further investigate how trait anxiety modulates the intra and internetwork coupling patterns, regression analysis for connectivity and trait anxiety was performed by controlling state anxiety. We finally used regression analysis to explore its relationship with drift rate.

Results

Effects of Long-Term Stress and Trait Anxiety on Psychological Distress

We first investigated how long-term stress and trait anxiety affect psychological distress. Participants' trait anxiety and psychological distress scores are listed in Supplementary Table S1. Two-sample *t*-test revealed higher psychological

distress in the stress than control group (t_{65} = 2.08, P = 0.041, d = 0.51) (Fig. 1c). Moreover, individuals with higher trait anxiety exhibited greater psychological distress within both the stress (r_{34} = 0.65, $P < 0.001$) and control groups (r_{29} = 0.41, P = 0.02) (Fig. 1d), even after regressing out state anxiety (stress: r_{34} = 0.48, P = 0.004, control: r_{29} = 0.47, P = 0.008) (Supplementary Fig. S3 and Table S2). Given the conventional regression or correlation models are sensitive to outliers and reflect only correlations with no predictive value, we then conducted machine learning-based prediction analyses mainly for the confirmatory purposes to confirm the robustness of results from above correlation analyses. Indeed, further prediction analyses confirmed that higher trait anxiety was predictive of greater distress after controlling for state anxiety in both groups (Supplementary Table S11).

Effects of Long-Term Stress on Cognitive Performance and Latent Dynamic Decision Measures

Next, we investigated how long-term stress affects general executive task-related performance and latent model-based parameters. Separate 2-by-2 ANOVAs were conducted for accuracy and average RTs with Group (stress vs. control) as between-subject factor and WM load (0- vs. 2-back) as within-subject factor. These analyses revealed a main effect of Group for RTs ($F_{1,66}$ = 5.37, P = 0.024, η^2_g = 0.06), which was mainly driven by faster RTs in the 2-back condition in the long-term stress group than controls ($t_{95.2}$ = −2.40, P = 0.018, d = −0.53), though this was less pronounced in the 0-back condition ($t_{95.2}$ = −1.77, P = 0.08, d = −0.49]. There was no main effect of Group on accuracy, nor Group-by-WM interactions for accuracy and RTs (all $F_{1,66} \leq 2.57$, $P \geq 0.11$).

We then investigated the effects of long-term stress on model-based measures by fitting the HDDM to trial-by-trial RTs separately for 0- and 2-back conditions across participants. The model comparisons were performed for a total of 15 plausible model variants (Supplementary Fig. S4). This yielded a model allowing for changes in parameters including drift rate v, decision threshold a, nondecision time t, and starting point z between conditions to provide the best fit and good convergence (Supplementary Table S3 and Fig. S5). Separate 2 (Group)-by-2 (WM-load) ANOVAs revealed a main effect of Group for drift rate ($F_{1,66}$ = 8.91, P = 0.004, η^2_g = 0.07) and decision-threshold ($F_{1,66}$ = 4.15, P = 0.046, η^2_g = 0.05). Compared with controls, individuals under long-term stress exhibited faster drift rate (t_{129} = 2.38, P = 0.019, d = 0.63) with comparable decision threshold (t_{83} = −1.44, P = 0.15, d = −0.40) in the 2-back condition, and faster drift rate (t_{129} = 2.17, P = 0.032, d = 0.49) but less stringent threshold (t_{83} = −2.39, P = 0.019, d = −0.52) in the 0-back condition. The statistics for other measures are provided in Supplementary Table S4. Together, these results indicate that long-term stress leads to faster drift rate and lower decision threshold compared with controls.

Long-Term Stress Shifts the Balance between WM-Related Brain Activation and Deactivation

We further investigated how long-term stress affects brain systems using whole-brain 2 (Group)-by-2 (WM-load) ANOVA. By contrasting the 2- with 0-back condition, we replicated robust WM-related activation and deactivation in core regions of the FPN and DMN, respectively (whole-brain family-wise error corrected $P < 0.05$) (Fig. 3a). Importantly, a contrast reflecting the main effect of Group revealed a hyper-activation in the anterior insula (Fig. 3b) and the middle occipital cortex (Supplementary Fig. S9) under long-term stress than controls (Supplementary Table S12) (voxel-wise $P < 0.001$, cluster $P < 0.05$ corrected). No correlation was found between drift rate and activation in the anterior insula (Supplementary Table S14). We also observed a Group-by-WM interaction in regions of the SN and DMN (Fig. 4a,b), with greater WM-related activation in the anterior insular and dACC in the long-term stress group than controls (voxel-wise $P < 0.005$, cluster $P < 0.05$ corrected) (Fig. 4b, Supplementary Table S13). For the DMN regions, we observed less WM-related deactivation in the MPFC and PCC in the long-term stress group than controls (Fig. 4a, Supplementary Table S13) (voxel-wise $P < 0.005$, cluster $P < 0.05$ corrected). These results indicate that long-term stress leads to hyper-activation in the SN regions, but less WM-deactivation in the DMN regions.

Long-Term Stress and Trait Anxiety Alter Latent Dynamic Decisions through Frontoparietal Activity

Since no direct associations of trait anxiety with RTs or drift rate were observed in either group (Supplementary Table S5), we then investigated whether trait anxiety modulates neural correlates of drift rate in the 2-back condition during which drift rate shows a long-term stress effect. Whole-brain independent sample t-test was conducted for the 2-back task-invoked activity maps between the 2 groups with drift rate as a covariate of interest. This analysis revealed a cluster in the IPS (voxel-wise $P < 0.005$, cluster $P < 0.05$ corrected), with higher task-invoked activity in this region associated with slower drift rate in the long-term stress group (r_{34} = −0.48, P = 0.003), but an opposite pattern in the control group (r_{30} = 0.40, P = 0.024) (Fig. 5a). Further analysis for Fisher's z-transformed correlations revealed a group difference (z = −3.71, $P < 0.001$, q = 0.95). When restricting our analysis to the stress group, we also observed a significant cluster in the MFG (voxel-wise $P < 0.005$, cluster $P < 0.05$ corrected), with higher task-invoked activity in this region associated with slower drift rate under long-term stress (r_{34} = −0.52, P = 0.001), but not in controls (r_{30} = 0.19, P = 0.31) (group difference: z = −3.02, P = 0.003, q = 0.77) (Fig. 5b). Prediction analyses confirmed that higher activity in the IPS and MFG was predictive of slower drift rate in the long-term stress group (Supplementary Table S11). No reliable correlation was observed for decision threshold with task-invoked brain activity during the 2-back condition.

We then observed positive correlations of trait anxiety with drift rate-related frontoparietal activity found above in the long-term stress group (IPS: r_{34} = 0.48, P = 0.003; MFG: r_{34} = 0.39, P = 0.02) but not controls (IPS: r_{30} = 0.11, P = 0.54; MFG: r_{30} = −0.14, P = 0.44) (Fig. 5a,b). Further tests revealed a group difference in correlations for the MFG (z = 2.16, P = 0.03, q = 0.41) but not IPS (z = 1.62, P = 0.11, q = 0.55). Prediction analyses confirmed that higher trait anxiety was predictive of higher activity in the IPS and MFG (Supplementary Table S11).

Given higher activity in the IPS and MFG were associated with higher trait anxiety and slower drift rate in the long-term stress group, 1 may conjuncture that task-invoked activity in these regions during the 2-back condition could act as a mediator to account for an indirect association between trait anxiety and drift rate. We thus implemented multigroup SEMs to test potential mediation effects of neural activity in the IPS and MFG in both 2 groups. These analyses revealed significant mediation effects of the frontoparietal activity (IPS: indirect Est. = −0.016, 95%CI = [−0.034,−0.006]; MFG:

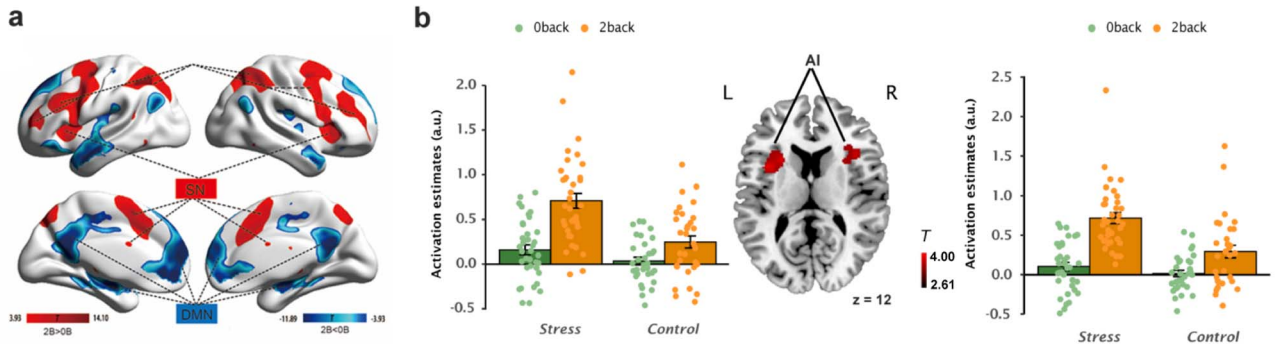

Figure 3. Brain regions showing main effects of WM load and long-term stress. (*a*) Significant clusters in distributed brain regions showing WM-related activation (red) and deactivation (blue) by contrasting 2- with 0-back conditions (whole-brain FWE $P < 0.05$ corrected). (*b*) Significant clusters in the bilateral anterior insula (middle) showing the main effect of long-term stress (voxel $P < 0.001$, and cluster $P < 0.05$ corrected) and corresponding parameter estimates extracted from the clusters. Color bar indicates minimum and maximal *T* values. Error bars represent standard error of the mean. Dots represent individual parameters.

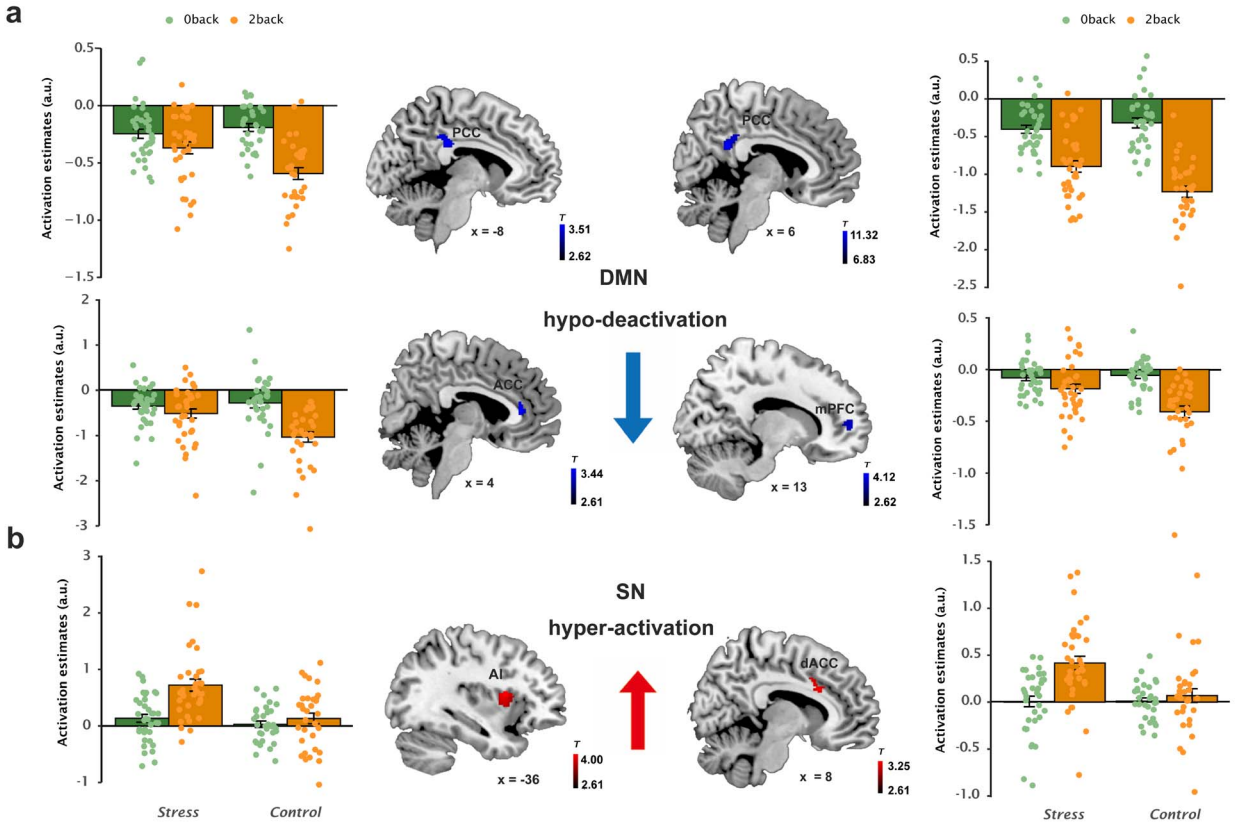

Figure 4. Long-term stress shifts the balance between WM-related brain activation and deactivation. The interaction effects between long-term stress and WM loads in brain regions of the DMN and SN. (*a*) Significant clusters in regions of the DMN including PCC and medial prefrontal cortex (middle), with weaker WM-related deactivation under long-term stress than control (voxel $P < 0.005$, cluster $P < 0.05$ corrected). Bar graphs depict corresponding parameter estimates only for visualization purpose. (*b*) Significant clusters in regions of the SN including the dACC and anterior insula (middle), with greater WM-related activation under long-term stress than controls (voxel $P < 0.005$, cluster $P < 0.05$ corrected). Bar graphs depict corresponding parameter estimates only for visualization purposes. Color bars indicate *T* values which vary from image-to-image. Error bars represent the standard error of mean. Dots represent individual data points.

indirect Est. = −0.013, 95%CI = [−0.029, −0.003]) on the indirect association between trait anxiety and drift rate under long-term stress (Fig. 5*a*, *b*) but not controls (Supplementary Fig. S7 and Supplementary Table S7). Critically, further analyses revealed significant group differences in the mediation effects for the IPS (Est. = −0.018, 95%CI = [−0.038, −0.005]) and MFG (Est. = −0.012, 95%CI = [−0.028, −0.001]). Parallel analyses for state anxiety, however, exhibited no group differences in the mediation effects for the IPS (Est. = −0.007, 95%CI = [−0.020,0.006]) and MFG (Est. = −0.008, 95%CI = [−0.025,0.003]) (Supplementary Table S8). Together, these results indicate that individuals with higher trait anxiety are prone to exhibit slower evidence accumulation

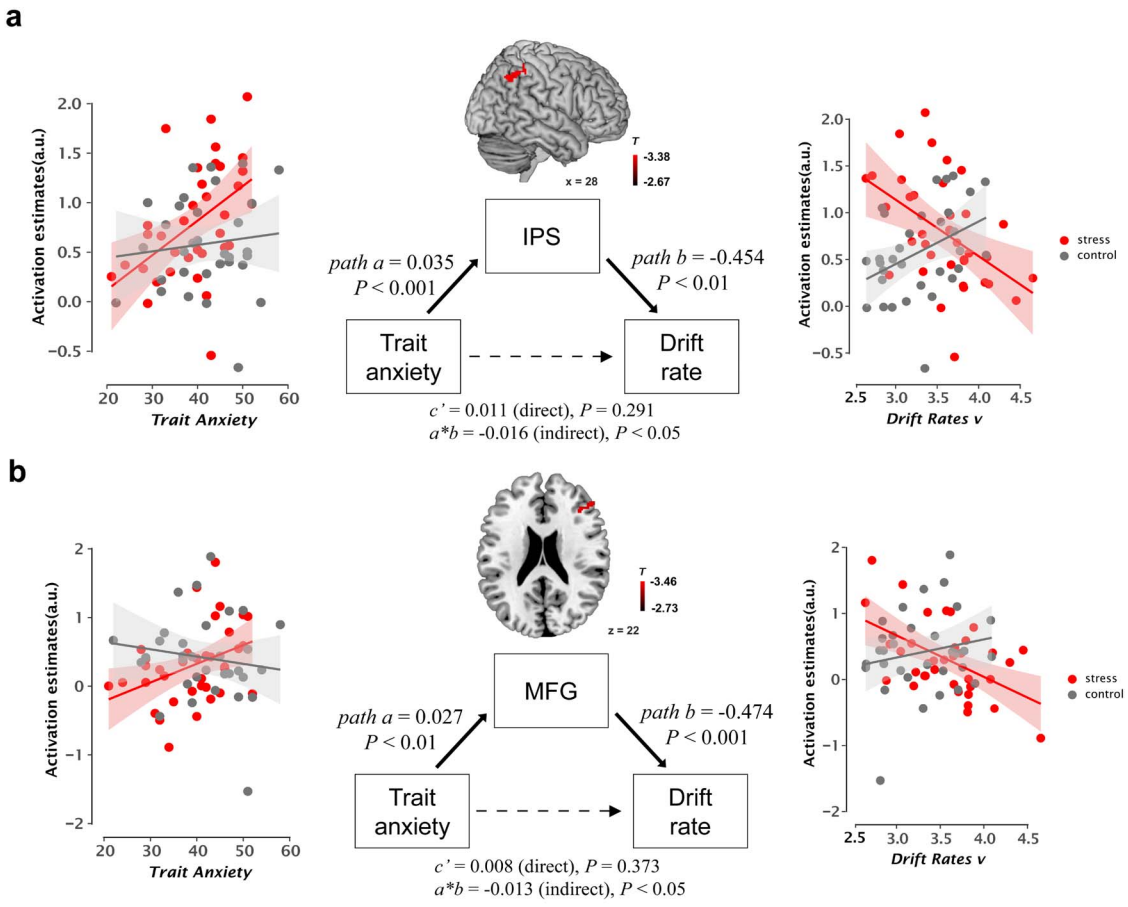

Figure 5. The relation between trait anxiety, brain activity, and drift rate. (*a*) Left and right: Scatter plots depict the correlations of individual's trait anxiety with executive function-related parietal activity which in turn was correlated with drift rate in the long-term stress and control groups. Middle: The mediating effect of executive function-related activity in the IPS on the relationship between trait anxiety and drift rate (voxel $P < 0.005$, cluster $P < 0.05$). (*b*) Left and right: Scatter plots depict the correlations of individual's trait anxiety with executive function-related prefrontal activity which in turn were correlated with drift rate in the long-term stress and control groups. Middle: The mediating effect of executive function-related activity in the middle frontal gyrus on the relationship between trait anxiety and drift rate (voxel $P < 0.005$, cluster $P < 0.05$). Color bar indicates minimum and maximal T values. Notes: $^{*}P < 0.05$, $^{**}P < 0.005$, $^{***}P < 0.001$.

than controls, mediated through higher frontalparietal activity during high-task demand under long-term stress.

Long-Term Stress and Trait Anxiety Alter Large-Scale Functional Brain Network Balance

To further investigate how long-term stress and trait anxiety affect functional coordination of large-scale brain networks during n-back task, we analyzed intra and internetwork coupling and decoupling among the FPN, DMN, and SN regions for each participant in the 2 groups. The FPN, DMN and SN nodes were independently defined to avoid selection biases (Fig. 6*a* and Supplementary Table S20). Separate 2 (Group)-by-2 (WM-load) ANOVA for intranetwork coupling revealed a main effect of WM-load for the FPN ($F_{1,66}$ = 4.17, $P = 0.045$, $\eta^2_g = 0.009$), but no long-term stress effects nor Group-by-WM interactions (Supplementary Table S21).

Parallel analyses for internetwork coupling revealed a main effect of WM-load for FPN–DMN decoupling and SN-DMN coupling (both $F_{1,66} > 4.67$, $P < 0.034$, $\eta^2_g = 0.05$ and 0.02 separately), and a main effect of Group ($F_{1,66}$ = 5.04, $P = 0.028$, $\eta^2_g = 0.05$) for FPN–DMN decoupling, with greater decoupling under long-term stress than controls ($t_{66} = -2.25$, $P = 0.028$, $d = -0.50$) (Fig. 6*b*). However, no Group-by-WM interaction was observed (Supplementary Table S21). Control analyses using nodes from meta-analysis of previous studies yielded similar effects (Supplementary Fig. S8). Critically, individuals with higher trait anxiety exhibited stronger FPN–DMN decoupling under long-term stress ($r_{34} = -0.36$, $P = 0.034$), but an opposite pattern in controls (r_{30} = 0.32, $P = 0.079$) in the 2-back condition after controlling for state anxiety (Fig. 6*c*). Prediction analyses confirmed that higher trait anxiety was predictive of stronger FPN–DMN decoupling under long-term stress (Supplementary Table S11). Further analysis revealed a significant group difference ($z = -2.78$, $P = 0.005$, $q = 0.71$), indicating a prominent interaction between trait anxiety and long-term stress on FPN–DMN decoupling. Interestingly, higher FPN–DMN decoupling was associated with lower drift rate in the stress group (r_{34} = 0.35, $P = 0.036$). These results indicate that long-term stress leads to increased FPN–DMN decoupling regardless of WM load, and higher trait anxiety is predictive of stronger FPN–DMN decoupling in those under long-term stress but not in controls under cognitively demanding task.

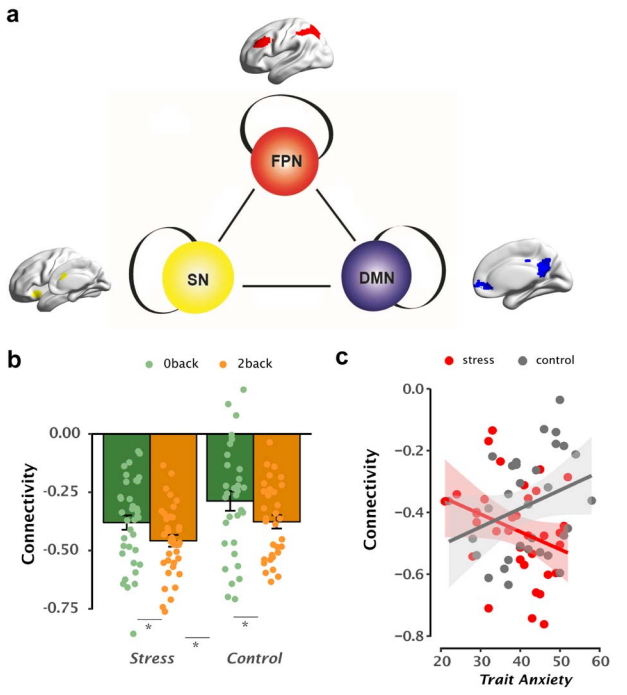

Figure 6. Internetwork connectivity modulated by trait anxiety under long-term stress. (*a*) Representative nodes of the 3 core brain networks involved in n-back processing, including the FPN, DMN, and SN. (*b*) Bar graphs depict the main effect of long-term stress on internetwork coupling between the FPN and DMN in 0-and 2-back conditions, with greater FPN–DMN decoupling in the long-term stress group in comparison to controls. (*c*) Scatter plot depicts an interaction effect between long-term stress and trait anxiety on FPN–DMN decoupling, with a negative correlation between decoupling strength and trait anxiety in the long-term stress group, but an opposite pattern in the control group. Solid lines represent the average, and shaded areas represent 95% confidence intervals. Dots represent individual data points.

Discussion

In this study, we investigated the neurocognitive mechanisms of how long-term stress and trait anxiety interact to affect dynamic decision computations during n-back task. We found that long-term stress led to higher psychological distress, faster RTs, and drift rate, but a lower decision-threshold than controls, with higher trait anxiety predictive of greater distress. These effects occurred with general hyper-activation in the anterior insula, greater WM-related activation in SN regions, and less WM-related deactivation in DMN regions. Moreover, individuals with higher trait anxiety were prone to slower drift rate via task-invoked activity in FPN regions under cognitively demanding task, in the long-term stress but not control group. Long-term stress also led to stronger DMN decoupling with the FPN than controls in high-task demand, with higher trait anxiety predictive of stronger FPN–DMN decoupling in those under long-term stress. Our findings provide a neurocognitive account for the interplay of long-term stress and trait anxiety on latent dynamic decisions during higher level cognitive task, via altered functional brain network balance among FPN, DMN, and SN regions.

As expected, individuals in the long-term stress group experienced higher psychological distress than controls, indicating the effectiveness of our natural long-term stress paradigm. Moreover, individuals with higher trait anxiety experienced more psychological distress in general, even after controlling for state anxiety. These results are in line with previous findings on sustained distress and other symptoms in chronic stress (MacLeod and Hagan 1992), which agrees with the psychological view of trait anxiety as a vulnerable phenotype of stress-related psychopathology (Bishop and Forster 2013; Weger and Sandi 2018). Behaviorally, individuals under long-term stress exhibited faster RTs but comparable accuracy than those in controls. Higher drift rate in the 2-back condition but a less stringent decision threshold in the 0-back condition was further observed by computational modeling of trial-by-trial decisive responses. In accordance with integrative models of stress, anxiety, and cognitive performance (Derakshan and Eysenck 2009; Edwards et al. 2015), our results show that sustained exposure to exam stress may not impair performance effectiveness (i.e., comparable accuracy), and may enhance processing efficiency (i.e., faster RTs and drift rate) under high-cognitive demanding task. However, such enhanced efficiency differs from previously reported cognitive deficits of chronic stress (Arnsten 2009; Lupien et al. 2009). Two factors are critical to reconcile this discrepancy. First, according to the Yerkes–Dodson law, the effects of stress on behavioral performance exhibit a nonlinear inverted-U shape curve as a function of stress severity and task difficulty. Thus, a beneficial effect can be reached at high levels of stress and task demands (Qin et al. 2012a). In this view, our observed faster RTs and drift rate may reflect enhanced processing efficiency at high-task demand in those under exam stress. Likewise, 1 previous study reported that stressed participants reacted faster at high-task demand (Schoofs et al. 2013).

Another factor is the interplay of long-term stress with trait anxiety that entails an individual's resilience and vulnerability to maladaptation (Ebner and Singewald 2017; Weger and Sandi 2018). When taking individual's trait anxiety into account, lower trait-anxious individuals exhibited relatively faster drift rate in those under long-term stress than in controls, whereas accuracy remained at a comparable level across groups and anxiety levels (Supplementary Fig. S6). In other words, stress-induced faster drift rate is driven by low-trait anxious individuals, suggesting that a beneficial form of adaptation to sustained exam stress is likely driven by enhanced processing efficiency in those individuals. This is consistent with previous studies on stress vulnerability reporting that some individuals seem to act as "resilient" agents who can develop adaptive strategies to cope with stress (Franklin et al. 2012; Ebner and Singewald 2017; Weger and Sandi 2018). Furthermore, our observations on high trait-anxious individuals may reflect the recruitment of compensatory strategies to prevent shortfalls in accuracy according to an influential model of cognitive trait anxiety and performance (Eysenck et al. 2007).

At the brain activation level, consistent with previous study (Phillips et al. 2008), individuals under long-term stress exhibited a general hyper-activation in the anterior insula regardless of WM load. Moreover, long-term stress led to greater WM-related activation in core nodes of the SN including the anterior insula and dACC, but less WM-related deactivation in the DMN regions. The anterior insula and dACC are thought to support salience processing, emotional awareness of distress, and executive function (Menon and Uddin 2010; Menon 2011). Based on the dual competition model of emotion-cognition interaction (Pessoa 2009), such SN regions are responsible for reallocating neural resources to resolve competition between emotional processing and executive function. Thus, greater SN

engagement under long-term stress may reflect recruitment of additional effort to cope with stress reactivity and to regulate stress-induced distress feelings along with related thoughts that are irrelevant to the WM task. Stress-induced task-irrelevant internal thoughts were indicated by accompanying less DMN deactivation, which parallels the empirical findings of aberrant DMN suppression in psychiatric diseases such as depression (Whitfield-Gabrieli and Ford 2012).

With respect to long-term stress and trait anxiety interactions on brain–behavior relationships, individuals with higher trait anxiety under long-term stress exhibited an indirect association with slower drift rate through higher frontoparietal activity but not those in controls under high-task demand. The lack of a mediation effect in the control group suggests that the FPN serves as a mediator only in individuals under long-term stress. Such mediation effects parallel the cognitive models of anxiety and related studies showing that high trait anxiety impairs processing efficiency but not performance effectiveness on tasks involving executive function under stressful conditions (Edwards et al. 2015). As discussed earlier, anxious individuals may recruit additional resources as a compensatory strategy to achieve comparable performance effectiveness (Calvo et al. 1994; Calvo 1996; Eysenck et al. 2007). Given the dlPFC and IPS have been associated with drift rate in the process of evidence accumulation in human and nonhuman primate studies with single cell recording (Sereno et al. 2001; Roitman and Shadlen 2002; Liu and Pleskac 2011), our observed higher frontoparietal engagement provides neuroimaging evidence to suggest that higher trait-anxious individuals under long-term stress tend to recruit more neural resources to maintain comparable task performance at the cost of the speed of evidence accumulation to make correct decisions when task demand increases. Specifically, unlike the 0-back condition that participants only respond to the stimuli that matches a prespecified number, thus sustained attention but no working memory demand is required. When performing the 2-back task under a normative condition, however, 1 must constantly update and maintain the most recent 2-items in mind and accumulate sufficient evidence extracted from each rapidly presented stimulus to ensure a correct decision whether the current item is a target or not (Ratcliff and Smith 2004). Under stress, however, high trait-anxious individuals experienced more distress likely with a hypervigilant state as indicated by hyper-activation in the SN. This might have impeded efficient extraction of target-relevant information due to potential confounds by feelings of distress, irrelevant thoughts, or other noise. Hence, more time is needed to suppress irrelevant information and accumulate sufficient evidence to reach a decision, thereby slowing the speed of evidence accumulation. Indeed, recent studies reported that the negative impact of trait anxiety extends beyond aversive feelings and involves impediment of ongoing goal-directed behaviors. This then results in an impaired capacity to disengage from the previously relevant sensory information to overcome distracting stimuli (Bishop 2007; Eysenck et al. 2007).

According to the neurobiological models of stress, the major targets of stress-sensitive hormones include regions of the FPN critical for drift rate during cognitively demanding task (Rasmussen et al. 1986). Given the link of high trait anxiety to stress sensitivity and stress hormone release (Bishop and Forster 2013), we thus speculate that excessive stress hormones might in part account for the higher activity in the IPS and MFG in trait-anxious individuals under long term-stress under cognitively demanding condition (i.e., 2-back). By extending such neurobiological accounts, our findings provide new insights suggesting that high trait anxiety per se does not necessarily lead to cognitive deficits. Rather, high trait anxiety works in concert with long-term stress to determine the (mal)adaptive effects on human brain and cognition. Together, under long-term stress, a slower speed of evidence accumulation in higher trait-anxious individuals may reflect less efficient evidence accumulation in the process of dynamic decisions during n-back when task load increases, likely via increased FPN engagement to make correct responses.

At the brain network level, we found greater FPN–DMN decoupling during WM under long-term stress than controls regardless of WM load. Stronger FPN–DMN decoupling here may reflect recruitment of additional effort to suppress task-irrelevant internal thoughts while performing the goal-directed task (Hampson et al. 2010; Liu et al. 2016). This notion is also in line with our observed faster RTs and drift rate under long-term stress. Critically, under high-task demand, individuals with higher trait anxiety exhibited stronger decoupling between DMN and FPN regions in those under long-term stress but not in controls, and such stronger decoupling was then associated with slower drift rate. This again provides evidence to suggest that high trait-anxious individuals might recruit additional resources relying on FPN–DMN decoupling, along with the elevated FPN activity mentioned above, to make correct responses and prevent a shortfall in accuracy at the cost of processing efficiency when task goal is difficult to achieve. Notably, the SN, especially the anterior insula and dACC, is thought to play a role in generating control signals to regulate switching between the FPN engagement in goal-directed tasks and DMN disengagement from irrelevant thoughts and mind wandering (Sridharan et al. 2008; Menon and Uddin 2010; Chen et al. 2013). Although we did not find effects of long-term stress and/or trait anxiety on SN coupling with other networks, this switching mechanism is still relevant to account for our observed hyper-activation of the SN, along with less WM-related deactivation in the DMN and the increased DMN-FPN decoupling under long-term stress. Such alterations in functional brain network balance may reflect shifted attention out of internally driven mental activity (i.e., stress-related distress feelings) to make correct decision during a cognitively demanding task.

It is worth noting that our observed effects of long-term stress and trait anxiety on neural activity and network coupling appear different in terms of the contrast of 2- versus 0-back condition and the 2-back condition only. Since WM-related effects are widely studied by contrasting a high against low-load condition, we thus feel that our observed effects in the 2-back condition might reflect executive functions with other components like selective attention and cognitive inhibition rather than WM alone. Indeed, executive functions contain 3 core components: working memory, inhibition and interference control (including selective attention and cognitive inhibition), and cognitive flexibility (Diamond 2013). When performing the 2-back task, in addition to constantly update and maintain the most recent 2-items in mind (i.e., the WM component of executive function), one also is needed to suppress irrelevant information and focus on target-relevant information to accumulate sufficient evidence extracted from each rapidly presented stimulus to ensure a correct decision (i.e., the selective attention and cognitive inhibition components of executive function). In addition, although trait and state anxiety are recognized as 2 distinct constructs in psychometric theory, they are intercorrelated and thus

challenging to dissociate. Nevertheless, our conclusions on trait anxiety still hold after controlling for state anxiety. Notably, the mediation effects of executive function-related frontoparietal activity on an indirect association between high trait anxiety and slower drift rate are only present in those under long-term stress. Such mediation effects are not present for those with higher state anxiety.

The following limitations should be considered. First, we only included male participants to mitigate potential confounds related to menstrual cycles (Etkin and Wager 2007), which limits the generalizability of our findings. Second, individual's intelligence may complicate our observed effects of long-term stress and trait anxiety on WM, though null effects of long-term stress or trait anxiety on WM accuracy may neutralize this concern. Third, individuals exposed to long-term exam stress might experience sleep disruption, other stressors, and a cognitive training that could complicate our findings. The involvement of a cognitive training, for instance, could account for faster RTs and drift rate under long-term stress than controls via improving cognitive functioning. Although this possibility concurs 1 form of aforementioned adaptive strategies participants developed to cope with exam stress, it cannot readily explain our major findings that high trait anxiety under long-term stress led to slower evidence accumulation through higher frontoparietal activity during high-task demand and increased decoupling between the default-mode and FPNs. Fourth, our block design for n-back task precludes trial-by-trial parametric modulation analyses for computational measures. Given a relatively small number of trials in our n-back task, we used the HDDM for its suitability to estimate model parameters across participants (Lerche et al. 2017). In fact, our validation analyses showed a good model fit as reported by previous studies (Cavanagh et al. 2014; O'Callaghan et al. 2017). Future studies with novel designs are needed to resolve these limitations.

In conclusion, our study demonstrates that long-term stress and trait anxiety interplay to affect latent dynamic decisions during n-back task by altering brain network balance in core regions of the SN, FPN, and DMN. Our findings point toward a neurocognitive model of how trait anxiety modulates latent decision-making dynamics during higher order executive functioning task under long-term stress, which may inform personalized assessments and preventions for stress-related (mal)adaptation.

Supplementary Material

Supplementary material can be found at *Cerebral Cortex* online.

Author Contributions

S.Q. and J.W. designed the research; G.H., J.W., C.L., Y.L., and J.L. performed the research; L.L. analyzed the data; L.L. and S.Q. wrote the manuscript.

Code availability

The scripts for this study are available at https://github.com/QinBrainLab/2018_stress_anxiety_brain.

Data availability

All the data used in this study are available from the corresponding author upon reasonable request.

Funding

National Natural Science Foundation of China (32130045, 31522028, 81571056, 82021004, 2014NT15, 31771246) and the Fundamental Research Funds for the Central Universities.

Notes

We thank the editor and anonymous reviewers for their valuable comments to improve the manuscript. We also thank Drs. Gang Chen, Baojuan Ye, Ling Wang, Hongyun Liu, and Junhao Pan for their advice on modeling and thresholding methods, and Drs. Christina Young and Peter Bayley for language editing. *Conflict of Interest*: None declared.

References

Arnsten AFT. 2009. Stress signalling pathways that impair prefrontal cortex structure and function. *Nat Rev Neurosci*. 10:410–422.

Birnbaum SG, Yuan PX, Wang M, Vijayraghavan S, Bloom AK, Davis DJ, Gobeske KT, Sweatt JD, Manji HK, Arnsten AFT. 2004. Protein kinase C Overactivity impairs prefrontal cortical regulation of working memory. *Science*. 306:882.

Bishop S, Forster S. 2013. Trait anxiety, neuroticism, and the brain basis of vulnerability to affective disorder. In: J. Armony & P. Vuilleumier, editor. *The Cambridge handbook of human affective neuroscience*. New York (NY: Cambridge University press. p. 553–574.

Bishop SJ. 2007. Neurocognitive mechanisms of anxiety: an integrative account. *Trends Cogn Sci*. 11:307–316.

Bishop SJ. 2009. Trait anxiety and impoverished prefrontal control of attention. *Nat Neurosci*. 12:92–98.

Browning M, Behrens TE, Jocham G, O'Reilly JX, Bishop SJ. 2015. Anxious individuals have difficulty learning the causal statistics of aversive environments. *Nat Neurosci*. 18:590–596.

Calvo MG. 1996. Phonological working memory and reading in test anxiety. *Memory*. 4:289–306.

Calvo MG, Eysenck MW, Ramos PM, Jiménez A. 1994. Compensatory reading strategies in test anxiety. *Anxiety Stress Coping*. 7:99–116.

Cavanagh JF, Wiecki TV, Kochar A, Frank MJ. 2014. Eye tracking and pupillometry are indicators of dissociable latent decision processes. *J Exp Psychol Gen*. 143:1476–1488.

Chen AC, Oathes DJ, Chang C, Bradley T, Zhou Z-W, Williams LM, Glover GH, Deisseroth K, Etkin A. 2013. Causal interactions between fronto-parietal central executive and default-mode networks in humans. *Proc Natl Acad Sci U S A*. 110:19944.

Cocchi L, Zalesky A, Fornito A, Mattingley JB. 2013. Dynamic cooperation and competition between brain systems during cognitive control. *Trends Cogn Sci*. 17:493–501.

Cohen J. 2013. *Statistical power analysis for the behavioral sciences*. New York: Academic Press.

Cohen JR. 2010. Decoding DEVELOPMENTAL differences and individual variability in response inhibition through predictive analyses across individuals. *Front Hum Neurosci*. 4:47.

Conway AR, Kane MJ, Bunting MF, Hambrick DZ, Wilhelm O, Engle RW. 2005. Working memory span tasks: a methodological review and user's guide. *Psychon B Rev*. 12:769–786.

de Kloet ER, Joëls M, Holsboer F. 2005. Stress and the brain: from adaptation to disease. *Nat Rev Neurosci*. 6:463–475.

Derakshan N, Eysenck MW. 2009. Anxiety, processing efficiency, and cognitive performance: new developments from attentional control theory. *Eur Psychol*. 14:168–176.

Derogatis LR, Unger R. 2010. Symptom checklist-90-revised. *Corsini Encyclopedia Psychol*. 1–2.

Diamond A. 2013. Executive functions. *Annu Rev Psychol*. 64:135–168.

Duan H, Yuan Y, Yang C, Zhang L, Zhang K, Wu J. 2015. Anticipatory processes under academic stress: an ERP study. *Brain Cogn*. 94:60–67.

Duan H, Yuan Y, Zhang L, Qin S, Zhang K, Buchanan TW, Wu J. 2013. Chronic stress exposure decreases the cortisol awakening response in healthy young men. *Stress*. 16:630–637.

Ebner K, Singewald N. 2017. Individual differences in stress susceptibility and stress inhibitory mechanisms. *Curr Opin Behav Sci*. 14:54–64.

Edwards EJ, Edwards MS, Lyvers M. 2015. Cognitive trait anxiety, situational stress, and mental effort predict shifting efficiency: implications for attentional control theory. *Emotion*. 15:350.

Etkin A, Wager TD. 2007. Functional neuroimaging of anxiety: a meta-analysis of emotional processing in PTSD, social anxiety disorder, and specific phobia. *Am J Psychiatry*. 164:1476–1488.

Eysenck MW, Derakshan N, Santos R, Calvo MG. 2007. Anxiety and cognitive performance: attentional control theory. *Emotion*. 7:336.

Franklin TB, Saab BJ, Mansuy IM. 2012. Neural mechanisms of stress resilience and vulnerability. *Neuron*. 75:747–761.

Hampson M, Driesen N, Roth JK, Gore JC, Constable RT. 2010. Functional connectivity between task-positive and task-negative brain areas and its relation to working memory performance. *Magn Reson Imaging*. 28:1051–1057.

Hayes AF, Preacher KJ, Myers TA. 2011. Mediation and the estimation of indirect effects in political communication research. *Sourcebook Polit Commun Res*. 23:434–465.

Hermans EJ, Henckens MJAG, Joëls FG. 2014. Dynamic adaptation of large-scale brain networks in response to acute stressors. *Trends Neurosci*. 37:304–314.

Hu L, Bentler PM. 1999. Cutoff criteria for fit indexes in covariance structure analysis: conventional criteria versus new alternatives. *Struct Equ Model Multidiscip J*. 6:1–55.

Joëls M, Pu Z, Wiegert O, Oitzl MS, Krugers HJ. 2006. Learning under stress: how does it work? *Trends Cogn Sci*. 10: 152–158.

Kane MJ, Engle RW. 2002. The role of prefrontal cortex in working-memory capacity, executive attention, and general fluid intelligence: an individual-differences perspective. *Psychon Bull Rev*. 9:637–671.

Lerche V, Voss A, Nagler M. 2017. How many trials are required for parameter estimation in diffusion modeling? A comparison of different optimization criteria. *Behav Res Methods*. 49:513–537.

Liston C, McEwen BS, Casey BJ. 2009. Psychosocial stress reversibly disrupts prefrontal processing and attentional control. *Proc Natl Acad Sci U S A*. 106:912.

Liu T, Pleskac TJ. 2011. Neural correlates of evidence accumulation in a perceptual decision task. *J Neurophysiol*. 106:2383–2398.

Liu Y, Lin W, Liu C, Wu J, Luo Y, Bayley PJ, Qin S. 2016. Memory consolidation reconfigures neural pathways involved in the suppression of emotional memories. *Nat Commun*. 7:1–12, 13375.

Luo Y, Qin S, Fernandez G, Zhang Y, Klumpers F, Li H. 2014. Emotion perception and executive control interact in the salience network during emotionally charged working memory processing. *Hum Brain Mapp*. 35:5606–5616.

Lupien SJ, McEwen BS, Gunnar MR, Heim C. 2009. Effects of stress throughout the lifespan on the brain, behaviour and cognition. *Nat Rev Neurosci*. 10:434–445.

MacLeod C, Hagan R. 1992. Individual differences in the selective processing of threatening information, and emotional responses to a stressful life event. *Behav Res Ther*. 30: 151–161.

McEwen BS, Morrison JH. 2013. The brain on stress: vulnerability and plasticity of the prefrontal cortex over the life course. *Neuron*. 79:16–29.

Menon. 2011. Large-scale brain networks and psychopathology: a unifying triple network model. *Trends Cogn Sci*. 15:483–506.

Menon V, Uddin LQ. 2010. Saliency, switching, attention and control: a network model of insula function. *Brain Struct Funct*. 214:655–667.

Mulder MJ, van Maanen L, Forstmann BU. 2014. Perceptual decision neurosciences – a model-based review. *Neuroscience*. 277:872–884.

Nichols T, Brett M, Andersson J, Wager T, Poline J-B. 2005. Valid conjunction inference with the minimum statistic. *Neuroimage*. 25:653–660.

O'Callaghan C, Hall JM, Tomassini A, Muller AJ, Walpola IC, Moustafa AA, Shine JM, Lewis SJG. 2017. Visual hallucinations are characterized by impaired sensory evidence accumulation: insights from hierarchical drift diffusion modeling in Parkinson's disease. *Biol Psychiatry*. 2:680–688.

Pessoa L. 2009. How do emotion and motivation direct executive control? *Trends Cogn Sci*. 13:160–166.

Phillips ML, Ladouceur CD, Drevets WC. 2008. A neural model of voluntary and automatic emotion regulation: implications for understanding the pathophysiology and neurodevelopment of bipolar disorder. *Mol Psychiatry*. 13:833–857.

Preacher KJ, Hayes AF. 2008. Asymptotic and resampling strategies for assessing and comparing indirect effects in multiple mediator models. *Behav Res Methods*. 40:879–891.

Qin S, Cousijn H, Rijpkema M, Luo J, Franke B, Hermans E, Fernández G. 2012a. The effect of moderate acute psychological stress on working memory-related neural activity is modulated by a genetic variation in catecholaminergic function in humans. *Front Integr Neurosci*. 6:1–12.

Qin S, Hermans EJ, van Marle HJF, Fernández G. 2012b. Understanding low reliability of memories for neutral information encoded under stress: alterations in memory-related activation in the hippocampus and midbrain. *J Neurosci*. 32:4032–4041.

Qin S, Hermans EJ, van Marle HJF, Luo J, Gn F. 2009. Acute psychological stress reduces working memory-related activity in the dorsolateral prefrontal cortex. *Biol Psychiatry*. 66:25–32.

Raichle ME, MacLeod AM, Snyder AZ, Powers WJ, Gusnard DA, Shulman GL. 2001. A default mode of brain function. *Proc Natl Acad Sci U S A*. 98:676.

Rasmussen K, Morilak DA, Jacobs BL. 1986. Single unit activity of locus coeruleus neurons in the freely moving cat: I. during naturalistic behaviors and in response to simple and complex stimuli. *Brain Res*. 371:324–334.

Ratcliff R. 1978. A theory of memory retrieval. *Psychol Rev*. 85:59–108.

Ratcliff R, Huang-Pollock C, McKoon G. 2018. Modeling individual differences in the go/no-go task with a diffusion model. *Decision*. 5:42–62.

Ratcliff R, McKoon G. 2007. The diffusion decision model: theory and data for two-choice decision tasks. *Neural Comput*. 20:873–922.

Ratcliff R, Smith PL. 2004. A comparison of sequential sampling models for two-choice reaction time. *Psychol Rev*. 111:333.

Roitman JD, Shadlen MN. 2002. Response of neurons in the lateral intraparietal area during a combined visual discrimination reaction time task. *J Neurosci*. 22:9475–9489.

Schoofs D, Pabst S, Brand M, Wolf OT. 2013. Working memory is differentially affected by stress in men and women. *Behav Brain Res*. 241:144–153.

Sereno M, Pitzalis S, Martinez A. 2001. Mapping of contralateral space in retinotopic coordinates by a parietal cortical area in humans. *Science*. 294:1350–1354.

Singmann H, Bolker B, Westfall J, Aust F, Højsgaard S, Fox J, Lawrence M, Mertens U, Love J. 2016. *Afex: analysis of factorial experiments. R package version 0.16-1. R package version 016 1*.

Spielberger CD. 1985. Assessment of state and trait anxiety: Conceptual and methodological issues. *Southern Psychologist*. 2(4):6–16.

Sridharan D, Levitin DJ, Menon V. 2008. A critical role for the right fronto-insular cortex in switching between central-executive and default-mode networks. *Proc Natl Acad Sci U S A*. 105:12569.

Wang M, Ramos BP, Paspalas CD, Shu Y, Simen A, Duque A, Vijayraghavan S, Brennan A, Dudley A, Nou E, et al. 2007. α2A-adrenoceptors strengthen working memory networks by inhibiting cAMP-HCN channel signaling in prefrontal cortex. *Cell*. 129:397–410.

Weger M, Sandi C. 2018. High anxiety trait: a vulnerable phenotype for stress-induced depression. *Neurosci Biobehav Rev*. 87:27–37.

Whitfield-Gabrieli S, Ford JM. 2012. Default mode network activity and connectivity in psychopathology. *Annu Rev Clin Psychol*. 8:49–76.

Whitfield-Gabrieli S, Nieto-Castanon A. 2012. Conn: a functional connectivity toolbox for correlated and anticorrelated brain networks. *Brain Connect*. 2:125–141.

Wiecki T, Sofer I, Frank M. 2013. HDDM: hierarchical Bayesian estimation of the drift-diffusion model in python. *Front Neuroinform*. 7:14.

Wu J, Yuan Y, Duan H, Qin S, Buchanan TW, Zhang K, Zhang L. 2014. Long-term academic stress increases the late component of error processing: an ERP study. *Biol Psychol*. 99:77–82.

Xiong B, Chen C, Tian Y, Zhang S, Liu C, Evans TM, Fernández G, Wu J, Qin S. 2021. Brain preparedness: The proactive role of the cortisol awakening response in hippocampal-prefrontal functional interactions. 205:102127.

Xu J, Hao L, Chen M, He Y, Jiang M, Tian T, Wang H, Wang Y, Wang D, Han ZR, Tan S, Men W, Gao J, He Y, Tao S, Dong Q, Qin S. 2021. Developmental Sex Differences in Negative Emotion Decision-Making Dynamics: Computational Evidence and Amygdala-Prefrontal Pathways, *Cerebral Cortex*, https://doi.org/10.1093/cercor/bhab359.

Yarkoni T, Poldrack RA, Nichols TE, Van Essen DC, Wager TD. 2011. Large-scale automated synthesis of human functional neuroimaging data. *Nat Methods*. 8:665–670.

Zhang J, Rittman T, Nombela C, Fois A, Coyle-Gilchrist I, Barker RA, Hughes LE, Rowe JB. 2015. Different decision deficits impair response inhibition in progressive supranuclear palsy and Parkinson's disease. *Brain*. 139:161–173.

Zhang J, Rowe JB. 2014. Dissociable mechanisms of speed-accuracy tradeoff during visual perceptual learning are revealed by a hierarchical drift-diffusion model. *Front Neurosci-Switz*. 8:69.